TÜBİTAK

Turkish Journal of Chemistry

http://journals.tubitak.gov.tr/chem/

Research Article

Turk J Chem
(2015) 39: 550 – 562

doi:10.3906/kim-1408-42

Encapsulation of copper(II) complexes with three dentate NO_2 ligands derived from 2,6-pyridinedicarboxylic acid in NaY zeolite

Massomeh GHORBANLOO[1,*], Somayeh GHAMARI[1], Hidenori YAHIRO[2]
[1]Department of Chemistry, Faculty of Science, University of Zanjan, Zanjan, Iran
[2]Department of Applied Chemistry, Faculty of Engineering, Ehime University, Matsuyama, Japan

Received: 16.08.2014 • **Accepted/Published Online:** 21.11.2014 • **Printed:** 30.06.2015

Abstract: 2,6-Pyridinedicarboxylic acid (H_2dipic) reacts with copper-exchanged zeolite NaY to form $[Cu(dipic)(H_2O)_2]_n$, which is encapsulated in the pores of the zeolite. In this zeolite-encapsulated form, the copper derivative functions as an efficient catalyst for the oxidation of cyclohexene, toluene, cyclohexane, and ethyl benzene in the presence of hydrogen peroxide (as an oxidant). The catalyst was readily recovered from the reaction mixture, and it could be reused for an additional three runs without perceptible loss of activity. The heterogeneous catalyst exhibited considerably higher activity and selectivity compared with $[Cu(dipic)(H_2O)_2]_n$ itself.

Key words: Encapsulated catalyst, zeolite, heterogeneous, hydrogen peroxide, copper complex

1. Introduction

Oxidation of olefins to give oxygen-containing value added products such as epoxides is a very important and valuable reaction in both the chemical and pharmaceutical industries.[1]

Most of such oxidation reactions are still via homogeneous catalysts, but deactivation of the catalyst by self-aggregation of active sites, high cost, and lack of recycling make them inappropriate for large-scale applications.[2] For overcoming these problems, heterogeneous catalysts with high activity and selectivity are potential candidates in comparison with their homogeneous counterparts.

Encapsulation of metal complexes inside the supercages of zeolites is a good method for heterogenizing catalysts.

Zeolites are crystalline, porous alumina silicates. The zeolitic cages are microscopically small.[3] Encapsulation of transition metal complexes in zeolite leads to transition metal complex molecules being encaged and site-isolated, and this can enhance the selectivity, activity, reusability, thermal, and chemical stability of the catalyst.[4,5]

In continuation of our previous research to expand well-organized heterogeneous catalysts to activate H_2O_2 to hydrocarbon oxidation,[2,6–8] we report here the synthesis of a copper(II) complex with H_2dipic and encapsulation of this complex in the cages of zeolite by the flexible ligand method.[9] Both homogeneous and heterogenized complexes, $[Cu(dipic)(H_2O)_2]_n$ and $[Cu(dipic)(H_2O)_2]_n$-Y, catalyzed the hydrocarbons in the presence of H_2O_2 as an oxidant without any co-catalyst.

*Correspondence: m_ghorbanloo@yahoo.com

2. Results and discussion

2.1. Preparation and characterization of the catalyst

The synthesis process of this heterogeneous catalyst, consistent with the flexible ligand method,[10] is shown in Scheme 1. The H_2dipic ligand could be inserted to the cavity of zeolite, owing to its flexibility, and reacted with metal ions exchanged into zeolite to form metal complex. For purification, the product, $[Cu(dipic)(H_2O)_2]_n$/Y, was washed several times with CH_2Cl_2, until excess ligands remaining uncomplexed in the cavities and on the external surface of the zeolite were completely removed. In addition, the $[Cu(dipic)(H_2O)_2]_n$/Y sample was ion-exchanged again with aqueous 0.1 mol L^{-1} NaCl solution to remove the uncomplexed copper(II) ions remaining in the zeolite.

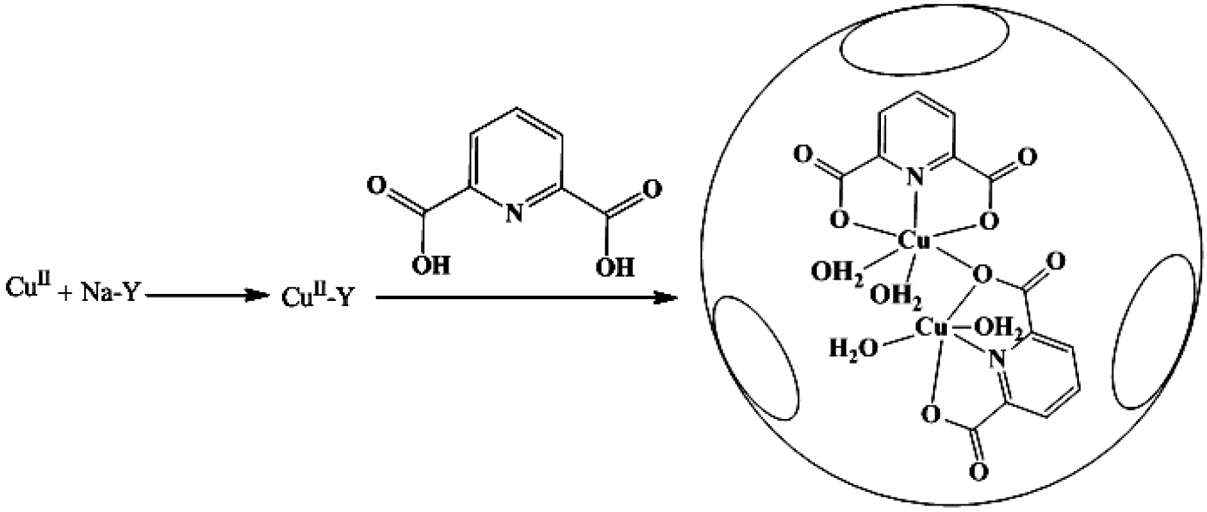

Scheme 1. Schematic representation of encapsulation of complex in the nanocavity of zeolite–Y.

The resulting catalyst was characterized by FTIR, XRD, and EPR. Figures 1a and 1b show the FTIR spectra of free ligand, H_2dipic, and its Cu^{II} complex, $[Cu(dipic)(H_2O)_2]_n$, respectively.

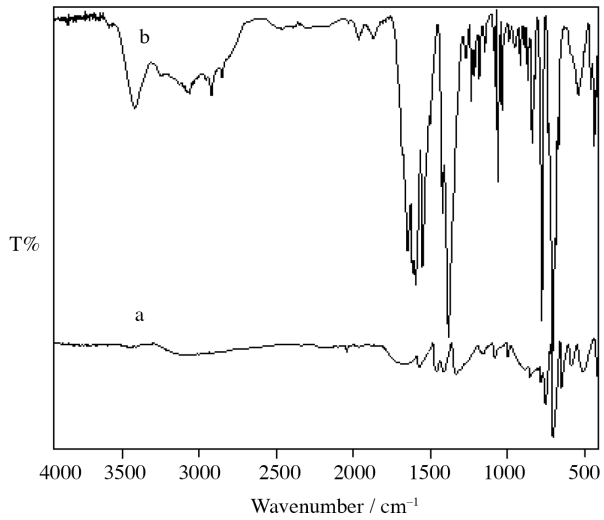

Figure 1. FTIR spectra of a) H_2dipic, b) $[Cu(dipic)(H_2O)_2]_n$.

The characteristic carboxyl vibration peaks of free 2,6-pyridinedicarboxylic acid ligand (Figure 1a) are at 1702 cm^{-1} (a strong and broad vibration) and 1341 and 1285 cm^{-1}, the first of which is assigned to the νC=O and the last two to the νC-O stretching vibrations;[11,12] moreover, pyridine ring (PR) bands are at 1581 and 1607 cm^{-1}.

The FTIR spectrum of the complex (Figure 1b) presents two distinguishable regions. In the high energy band region, ranging from 3500 to 2700 cm^{-1}, there are absorption peaks at near 3430 cm^{-1}, due to νOH of free water molecules. In the low energy band scope, a series of absorption peaks were observed, such as νC=O at 1651 cm^{-1}, νPR at 1602 and 1620 cm^{-1} (PR = Py ring), δOH at 961 cm^{-1}, and δCH at 1384 and 841 cm^{-1},[13] and strong to medium bands at ~436 and ~545 cm^{-1} attributed to ν(M–N) and ν(M–O), respectively, were observed for the complex.[14] The evaluation of the FTIR spectra of free ligand and its Cu^{II} complex (Figures 1a and 1b, respectively) enables the confirmation for the coordination mode of the ligand.

FTIR spectroscopy provides information on the integrity of the encapsulated complexes, in addition to the crystallinity of the host zeolite. The FTIR bands of encapsulated complexes are weak due to their low concentration in the zeolite, and therefore can only be observed in the regions where the zeolite matrix does not give intense bands, from 1200 to 1640 cm^{-1}. It also can be seen that significant bands were obtained at about 3090 cm^{-1} in the spectra of the $[Cu(dipic)(H_2O)_2]_n$/Y, which are assigned to aromatic C–H vibrations of the ligand. In contrast, these bands were absent for the Na–Y sample. In addition, the band observed at 1634 cm^{-1} is related to the bending vibration of H_2O molecules in the zeolite lattice in all the spectra. As shown in Figures 2a and 2b, the shifts of wavenumber and the changes in the relative intensity of the vibration bands prove guest/host interactions. These observations suggest not only the presence of copper^{II} complex in the zeolite, but also the presence of interactions between the copper^{II} complex and the zeolite matrix.

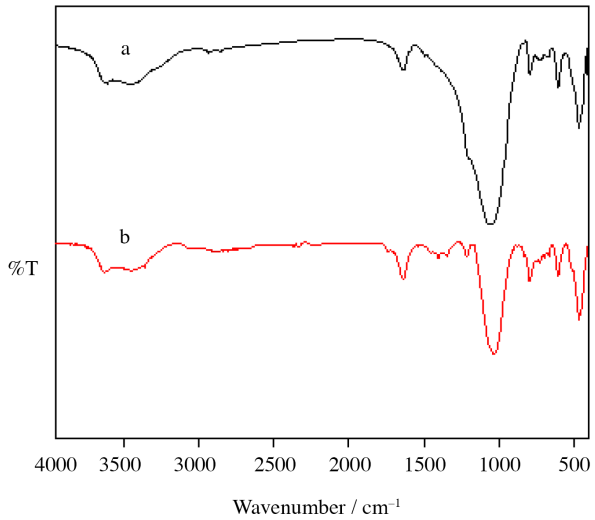

Figure 2. FTIR spectra of a) Na–Y, b) $[Cu(dipic)(H_2O)_2]_n$/Y.

The EPR spectrum of the neat copper complex, $[Cu(dipic)(H_2O)_2]_n$, was recorded at room temperature (Figure 3a). The EPR spectrum of $[Cu(dipic)(H_2O)_2]_n$ consisted of a broad isotropic signal centered at g_{iso} = 2.11. No hyperfine structure due to Cu (I = 3/2) was observed because of the higher concentration of copper.

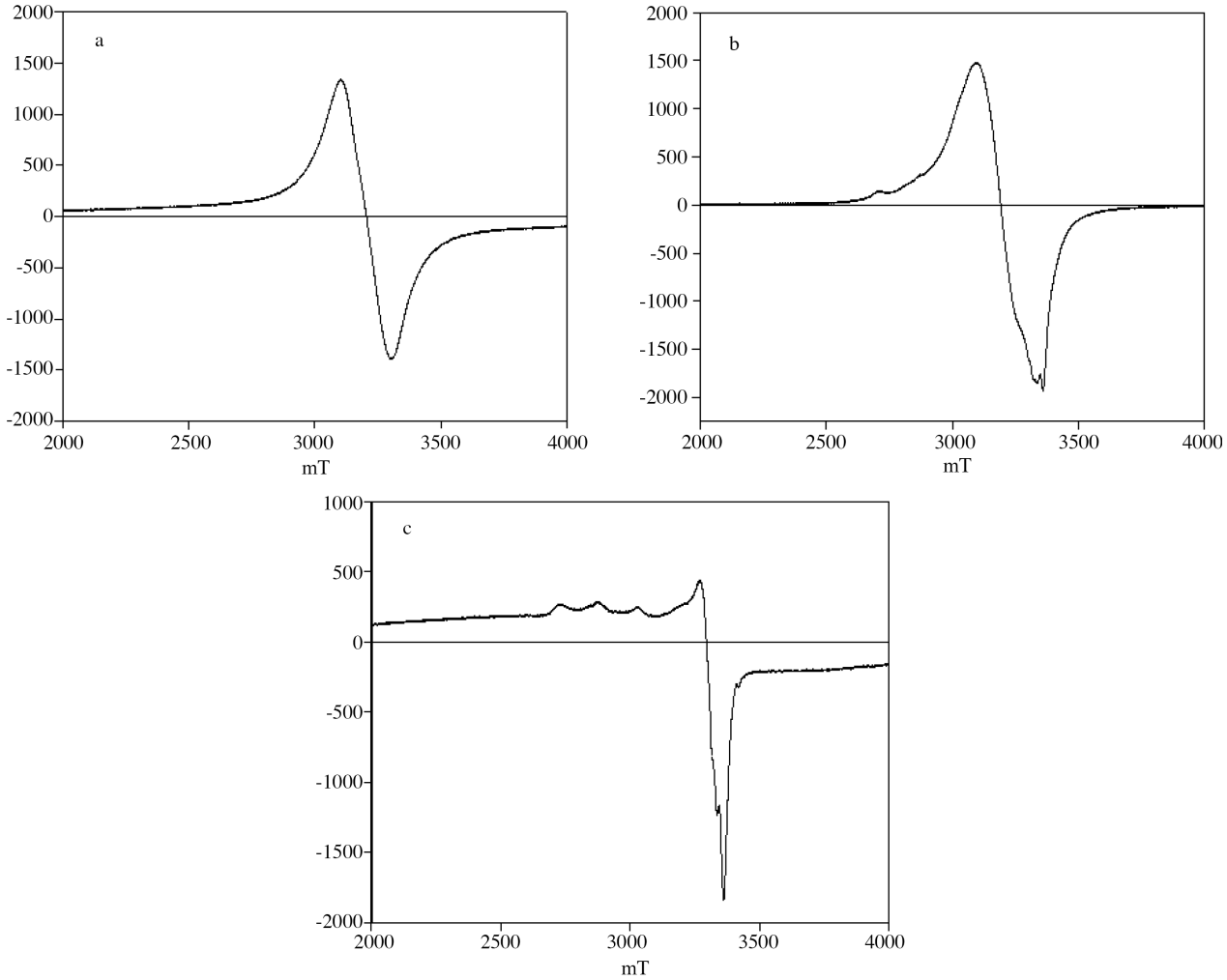

Figure 3. EPR spectra of a) $[Cu(dipic)(H_2O)_2]_n$, b) Cu/Y and c) $[Cu(dipic)(H_2O)_2]_n$/Y.

Cu^{II}–Y exhibited an EPR spectrum (Figure 3b) composed of two different signals: one is a broad singlet signal with $g_{iso} = 2.11$ due to the strong interaction among Cu^{II} ions located close to one another and the other is the axially symmetric signals attributed to isolated Cu^{II} ion. l The EPR spectrum of $[Cu(dipic)(H_2O)_2]_n$/Y exhibited well resolved hyperfine couplings in the region of 250–350 mT (Figure 3c). The $g_{||}$ and g $\perp$ values of $[Cu(dipic)(H_2O)_2]_n$/Y can be estimated to be 2.29 and 2.05, respectively.

The hyperfine coupling constant of the parallel component was 15 mT. The shifting of EPR line of $[Cu(dipic)(H_2O)_2]_n$/Y to the higher field region in comparison to the corresponding line of Cu^{II}–Y is probably due to the increase in ligand field around the Cu(II) ion on encapsulation.[15,16] No signals due to isolated Cu^{II} ions in Cu–Y and no broad singlet signal suggest Cu(II) ions formed the complexes[17] in the $[Cu(dipic)(H_2O)_2]_n$/Y. As can be seen in the ESR spectrum of $[Cu(dipic)(H_2O)_2]_n$/Y, a weak signal was observed in the half-field region ($\Delta MS = \pm 2$), indicating a binuclear complex with ferromagnetic coupling of the unpaired spins of two Cu^{II} ions in binuclear complexes resulting in an S = 1 ground state. The transitions at $g \approx 4$ could be assigned to ferromagnetic coupling of Cu^{II}–Cu^{II} dimers[18–22] and Fe impurity in the zeolite matrix in the heterogeneous complex.[23]

The X-ray powder diffraction patterns of Na/Y and $[Cu(dipic)(H_2O)_2]_n$/Y are shown in Figures 4a and 4b, respectively. The XRD peaks of $[Cu(dipic)(H_2O)_2]_n$/Y were similar to those of Na/Y except for a minor change in the intensity of the peaks and no new crystalline pattern emerged. These facts demonstrated that the framework and crystallinity of zeolite were not damaged during the preparation, and that the complexes were well dispersed in the cages. It is known that the relative peak intensities of the (2 2 0), (3 1 1), and (3 3 1) reflections are related to the locations of cations. In Na/Y without complex, the order of peak intensity was $I_{331} >> I_{220} > I_{311}$, while in encapsulated complexes, the order of peak intensity was $I_{331} >> I_{311} > I_{220}$. The difference indicates that Cu^{II} ion exchanged with Na+ ion undergoes rearrangement in complexation.[24] New peaks due to complex encapsulated in zeolite were detected probably due to the very low loading amount of metal complex.

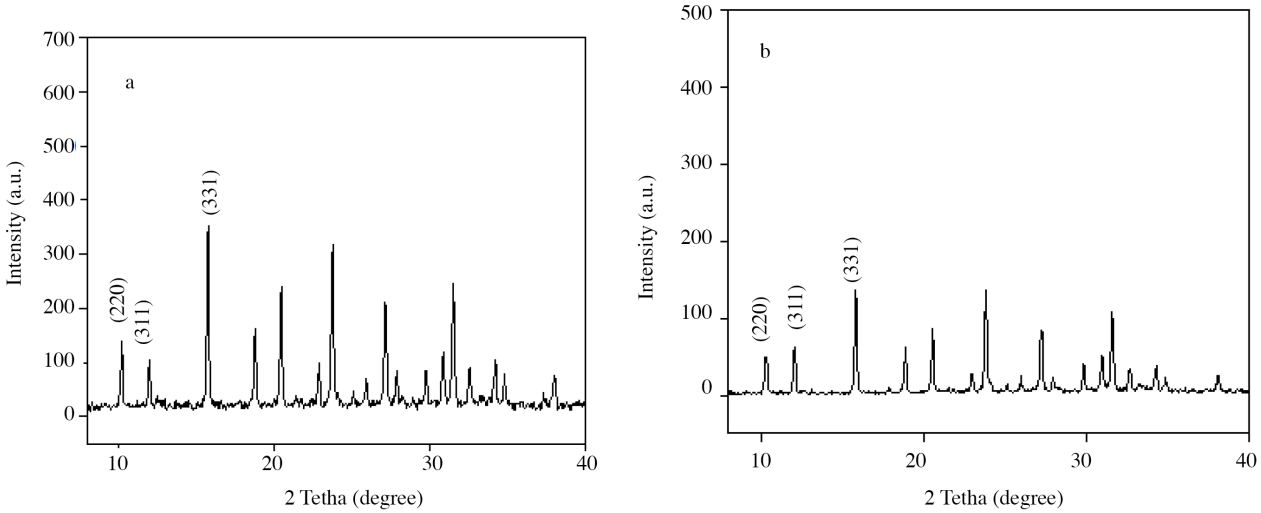

Figure 4. XRD spectra a) zeolite, b) $[Cu(dipic)(H_2O)_2]_n$/Y.

2.2. Catalytic activity

The $[Cu(dipic)(H_2O)_2]_n$ catalyst was used in the oxidation of cyclohexene using 30% aqueous H_2O_2 as the oxidant and acetonitrile as the solvent, at 60 °C, and the results are listed in Table 1.

Table 1. Catalytic activity of $[Cu(dipic)(H_2O)_2]_n$ on cyclohexene oxidation.[a]

Entry	$[H_2O_2]/[C_6H_{10}]$ Molar ratio	Solvent	Temperature (°C)	Conversion (%)	Epoxide (%) selectivity (%)
1	1	CH_3CN	60	17.5	79 [b]
2	2	CH_3CN	60	40	88 [b]
3	3	CH_3CN	60	78	93 [b]
4	4	CH_3CN	60	79	91 [b]
5	3	MeOH	60	38.5	85 [b]
6	3	EtOH	60	33	68 [b]
7	3	n-Hexane	60	0	—
8	3	CH_3CN	40	10	89 [b]
9	3	CH_3CN	80	57	87 [b]

[a] Reaction conditions: catalyst $[Cu(dipic)(H_2O)_2]_n$) 4 mg (0.015 mmol catalyst); cyclohexene, 1 mmol; solvent, 2 mL; reaction time, 4 h; b) 2-cyclohexen-1-ol as the other product.

Control experiments show that both catalyst and the oxidant are essential to the oxidation process, as seen from the experiments on the homogeneous catalyst $[Cu(dipic)(H_2O)_2]_n$ in the oxidation of cyclohexene to cyclohexene epoxide at 60 °C; 30% aqueous hydrogen peroxide served as the oxidant and actonitrile the solvent (Table 1). The oxidation of cyclohexene in the absence of H_2O_2 did not occur, whereas in the absence of a catalyst the oxidation only proceeded by up to 6% after 24 h.[6,25,26]

In order to optimize the reaction conditions for yielding maximum conversion of cyclohexene, the effects of H_2O_2 concentration (mol of H_2O_2 per mol of cyclohexene), temperature, and solvent on the catalytic activity were investigated.

The conversion increased when more hydrogen peroxide was used.

The nature of the solvent was found to have a marked effect (Table 1, entries 3, 5–7).

The catalytic activity decreased in the following order: acetonitrile (dielectric constants ($\varepsilon/\varepsilon_0 = 37.5$) > methanol ($\varepsilon/\varepsilon_0 = 32.7$) > ethanol ($\varepsilon/\varepsilon_0 = 24.3$) > n-hexane ($\varepsilon/\varepsilon_0 = 1.88$). The highest conversion was obtained in acetonitrile (78% after 4 h). This may be attributable to the high relative dielectric constant and dipole moment ($\mu = 3.90$ D) of acetonitrile. The optimum polarity of acetonitrile helps to dissolve both the alkenes and H_2O_2, which facilitates the epoxidation reaction in this solvent. In addition, n-hexane is immiscible with aqueous H_2O_2; for this reason, catalytic efficiency is decreased in this solvent.

Temperature had a distinguished effect on the conversion of cyclohexene in the range from 40 to 80 °C (Table 1, entries 3, 8, and 9). The conversion of cyclohexene was increased with increasing reaction temperature from 40 to 60 °C (Table 1, entries 3 and 8); moreover, selectivity is strongly dependent on temperature. At above 60 °C, conversion was decreased (Table 1, entry 9). This may be caused by an increase in the rate of H_2O_2 decomposition at higher temperature. Furthermore, at higher temperature, the selectivity to cyclohexene epoxide as a main product of cyclohexene oxidation rapidly declined, whereas the selectivity to other products such as 2-cyclohexen-1-ol increased.

The oxidation reactions of cyclohexane, toluene, and ethyl benzene over $[Cu(dipic)(H_2O)_2]_n$ were also examined. To attain appropriate reaction conditions for maximum alteration of cyclohexane, H_2O_2 concentration (mol of H_2O_2 per mol of cyclohexane) and temperature were studied.

The effect of H_2O_2 concentration on the cyclohexane oxidation reaction is shown in Table 2, entries 1–4.

Table 2. Catalytic activity of $[Cu(dipic)(H_2O)_2]_n$ on cyclohexane oxidation.[a]

Entry	H_2O_2:substrate molar ratio	Temperature (°C)	Conversion[b] (%)	Selectivity (%) Cyclohexanol/cyclohexanone
1	1:1	60	5	94/6
2	2:1	60	17	95/5
3	3:1	60	34	92/8
4	4:1	60	48	86/14
5	4:1	40	10	95/5
6	4:1	80	32	75/25

[a] Reaction conditions: Catalyst ($[Cu(dipic)(H_2O)_2]_n$) 4 mg (0.015 mmol catalyst); Cyclohexane, 1 mmol; acetonitrile, 2 mL; reaction time, 4 h, [b] Conversions are based on the starting substrate.

The effect of temperature is also shown in Table 2. The conversion of cyclohexane was increased from 40 to 60 °C (Table 2, entries 4–6), but at higher temperature H_2O_2 was decomposed. Moreover, at higher temperature, the selectivity to cyclohexanone increased.

The oxidation of ethyl benzene, toluene, cyclohexene, and cyclohexane over $[Cu(dipic)(H_2O)_2]_n$ and $[Cu(dipic)(H_2O)_2]_n$/Y catalysts was carried out under the optimized conditions. As can be seen in Table 3, acetophenone was formed as a major product, while benzaldehyde and benzoic acid were generated as minor ones. Thus side-chain oxidation was observed.

Table 3. Oxidation of hydrocarbons by the $[Cu(dipic)(H_2O)_2]_n]$ (**1**) and $[Cu(dipic)(H_2O)_2]_n$/Y (**2**).[a]

Entry	Hydrocarbon	Conversion (%)[b] **(1)/(2)**	Selectivity (%) **(1)/(2)**						
			BA	AP	BAc	BAlc	epox	alcohol	keton
1	Ethyl benzene	37 /42	2 / 0	98 / 88	0 / 12	—	—	—	—
2	Toluene	25 / 31	13 / 59	—	1 / 10	86 / 31	—	—	—
3	Cyclohexane	48 / 56	—	—	—	—	—	86 / 38	14 / 62
	Cyclohexene	78 / 90	—	—	—	—	93 / 78	7 / 20	–/2

[a] Reaction conditions: catalyst: $((Fe_3O_4@SiO_2/[Cu(tyr)_2]_n)$ (**2**) (0.0023 mmol catalyst), $([Cu(tyr)_2]_n$ (**1**)) (0.0023 mmol)); substrate 1.0 mmol, CH_3CN 2 mL, H_2O_2 4 mmol, $NaHCO_3$ 0.5 mmol, temperature 60 ± 1 °C and time 2 h (For heterogeneous catalyst)/4 h (For homogeneous catalyst); [b] Conversions are based on the starting substrate for heterogeneous/homogeneous conditions; BA = benzaldehyde; BAlc = benzyl alcohol; BAc = benzoic acid; AP = acetophenone

The oxidation of toluene takes place on the side chain of the toluene (Table 3, entry 2) and the selectivity to benzyl alcohol was higher than that to other products.

A salient difference in selectivity between $[Cu(dipic)(H_2O)_2]_n$ and encapsulated $[Cu(dipic)(H_2O)_2]_n$/Y was seen in the oxidation of all substrates (Table 3, entries 1–4). The oxidation rate obtained with $[Cu(dipic)(H_2O)_2]_n$/Y was higher than that with the homogeneous catalyst, similar to that reported in Mn–Me_3tacn complex in zeolites.[27] The ratio of cyclohexene epoxide/2-cyclo-hexene-1-ol was 6 for the $[Cu(dipic)(H_2O)_2]_n$/H_2O_2 system; however, its heterogeneous counterpart produced the same products in 0.6 of the ratio of cyclo-hexene epoxide/2-cyclo-hexene-1-ol. The effect of zeolite-Y on complex activity was reflected in the oxidation of all substrates. Both $[Cu(dipic)(H_2O)_2]_n$ and encapsulated $[Cu(dipic)(H_2O)_2]_n$/Y catalysts oxidized toluene and ethyl benzene to benzyl alcohol/benzaldehyde/benzoic acid and acetophenone/benzaldehyde/benzoic acid, respectively, with different activity and selectivity (Table 3, entries 1 and 2). This is due to the site isolation effect, which makes the complex a molecularly dispersed form, resulting in no self-degradation. In terms of time period, when $[Cu(dipic)(H_2O)_2]_n$/Y is used in place of $[Cu(dipic)(H_2O)_2]_n$, the reaction time is decreased from 4 h to only 2 h.

In Table 4, our catalyst is compared with the literature catalysts.

Compared with the earlier reported catalysts, the $[Cu(dipic)(H_2O)_2]_n$ and $[Cu(dipic)(H_2O)_2]_n$/Y exhibited superior activity for the oxidation of hydrocarbons. Cu–salen[28], Cu–salen/Y[28], Cu–[H_4]salen[28], and Cu–[H_4]salen/Y[28] showed lower catalytic activity in the oxidation of cyclohexane. Moreover, our catalysts showed higher catalytic activity than the Y–[Cu(Me_2salen)][29] and $[Cu([CH_3]_2–N_2S_2)]^{2+}$–NaY[30] in oxidation of ethyl benzene. Furthermore, our homogeneous and heterogeneous catalysts are very efficient compared to $[Cu(H_4C_6N_6S_2)]$–NaY[31] in the oxidation of cyclohexene. In addition, the catalyst and method applied in this paper have advantages in terms of heterogeneous nature, high reusability, high conversions, and selectivity of the catalyst.

2.3. Catalyst recycling

The heterogeneous catalyst ($[Cu(dipic)(H_2O)_2]_n$/Y) could be used for a third run (Table 5) and noticeable decreases in activity was observed.

Table 4. Comparison of literature catalysts and our catalyst system for oxidation of hydrocarbons.

Entry	Catalyst	Reaction condition	Substrate	Conversion (%)
1	Cu–salen[28]	Reaction conditions: 0.1 g catalyst (0.01 mmol for pure complexes), 10 mL CH_3CN, 18.5 mmol cyclohexane, 19.5 mmol H_2O_2 (30% in aqueous solution), 60 °C, 2 h.	Cyclohexane	6.1
2	Cu–salen/Y[28]	Reaction conditions: 0.1 g catalyst (0.01 mmol for pure complexes), 10 mL acetonitrile, 18.5 mmol cyclohexane, 19.5 mmol H_2O_2 (30% in aqueous solution), 60 °C, 2 h.	Cyclohexane	4
3	Cu–[H_4]salen[28]	Reaction conditions: 0.1 g catalyst (0.01 mmol), 10 mL CH_3CN, 18.5 mmol cyclohexane, 19.5 mmol H_2O_2 (30% in aqueous solution), 60 °C, 2 h.	Cyclohexane	7.9
4	Cu–[H_4]salen/Y[28]	Reaction conditions: 0.1 g catalyst (0.01 mmol for pure complexes), 10 mL CH_3CN, 18.5 mmol cyclohexane, 19.5 mmol H_2O_2 (30% in aqueous solution), 60 °C, 2 h.	Cyclohexane	9.5
5	$[Cu(dipic)(H_2O)_2]_n$] / $[Cu(dipic)(H_2O)_2]_n$]/Y[This work]	$[Cu(dipic)(H_2O)_2]_n$] (**1**)) (0.015 mmol), (($[Cu(dipic)(H_2O)_2]_n$/Y) (**2**) (0.015 mmol (0.038 g) catalyst); substrate 1.0 mmol, CH_3CN = 2 mL, H_2O_2 4 mmol, temperature 60 ± 1 °C and time 4 h (For homogeneous catalyst) /2 h (For heterogeneous catalyst)	Cyclohexane	48 / 56
6	Y-Cu(dmgH)$_2$[29]	Reaction conditions: ethylbenzene = 0.03 mol; catalyst = 50 mg, H_2O_2 = 0.06 mol; Benzene (solvent) = 10 mL; temperature = 323 K.	Ethyl benzene	24
7	Y-CuMe$_2$salen[29]	Reaction conditions: ethylbenzene = 0.03 mol; catalyst = 50 mg, H_2O_2 = 0.06 mol; Benzene (solvent) = 10 mL; temperature = 323 K.	Ethyl benzene	23
8	$[Cu([CH_3]_2\text{-}N_2S_2)]^{2+}$–NaY[30]	Reaction conditions: ethylbenzene = 0.105 g (1 mmol); catalyst = 0.004 mmol; 50% TBHP in ethylenedichloride = 0.42 ml; CH_3CN = 1 mL; temperature = 333 K	Ethyl benzene	30
9	$[Cu(dipic)(H_2O)_2]_n$] / $[Cu(dipic)(H_2O)_2]_n$]/Y[This work]	$[Cu(dipic)(H_2O)_2]_n$] (**1**)) (0.015 mmol), (($[Cu(dipic)(H_2O)_2]_n$/Y) (**2**) (0.015 mmol (0.038 g) catalyst); substrate 1.0 mmol, CH_3CN = 2 mL, H_2O_2 4 mmol, temperature 60 ± 1 °C and time 4 h (For homogeneous catalyst) /2 h (For heterogeneous catalyst)	Ethyl benzene	37 / 42
10	[[$Cu(H_4C_6N_6S_2)$]–NaY[31]	Reaction conditions: catalyst = 1.02×10^{-5} mol, Cyclohexene, TBHP = 16 mL; CH_2Cl_2 = 10 mL; temperature = 25 °C, 8 h, under N_2 atmosphere.	Cyclohexene	40
11	$[Cu(dipic)(H_2O)_2]_n$] / $[Cu(dipic)(H_2O)_2]_n$]/Y[This work]	$[Cu(dipic)(H_2O)_2]_n$] (**1**)) (0.015 mmol), (($[Cu(dipic)(H_2O)_2]_n$/Y) (**2**) (0.015 mmol (0.038 g) catalyst); substrate 1.0 mmol, CH_3CN = 2 mL, H_2O_2 4 mmol, temperature 60 ± 1 °C and time 4 h (For homogeneous catalyst) /2 h (For heterogeneous catalyst)	Cyclohexene	78 / 90

Table 5. Effect of catalyst recycling on cyclohexene oxidation.[a]

Recycle number	Conversion (%)	Epoxide selectivity (%)	
Fresh	78	93	7
1	77	92	8
2	78	93	7
3	77	91	9

[a] Reaction conditions: a) catalyst ($[Cu(dipic)(H_2O)_2]_n$/Y) ((0.038 g) (0.015 mmol catalyst); cyclohexene, 1 mmol; solvent, 2 mL; reaction time, 2 h; H_2O_2, 3 mmol.

After one reaction run, the catalyst was recovered by the centrifugation of a hot reaction mixture in order to prevent the re-adsorption of possibly leached complex molecules, and additionally washed with acetonitrile and dried at 80 °C. The dried sample was then used for the next run under the same reaction conditions. Table 5 shows the catalytic results of three successive recycles.

It is clear that the cyclohexene conversion was virtually the same in the three reaction runs, proving that $[Cu(dipic)(H_2O)_2]_n$/Y is highly stable and can be reused. On the whole, no noteworthy loss in catalytic activity was observed compared with that of a fresh sample, as shown in Table 5. Thus, catalyst recycling is possible.

2.4. Catalyst stability

In the oxidation of cyclohexene by **2**, the catalyst was separated by filtration after 1 h (at which the conversion was 40%). GC analysis of the filtrate after the filtrate was set aside for another hour showed conversion of 47%. The 7% difference increase in the conversion of cyclohexene is related to oxidation in the absence of the catalyst, which had already been removed (control reactions). If the copper complex was indeed leached,[32] then copper should be detected by atomic absorption spectroscopy. However, the AA results are inconsistent with leaching as the quantity was less than 0.03 ppm. The catalyst, when reused in a subsequent run, displayed an identical FTIR spectrum compared with one that had not been used (Figure 5).

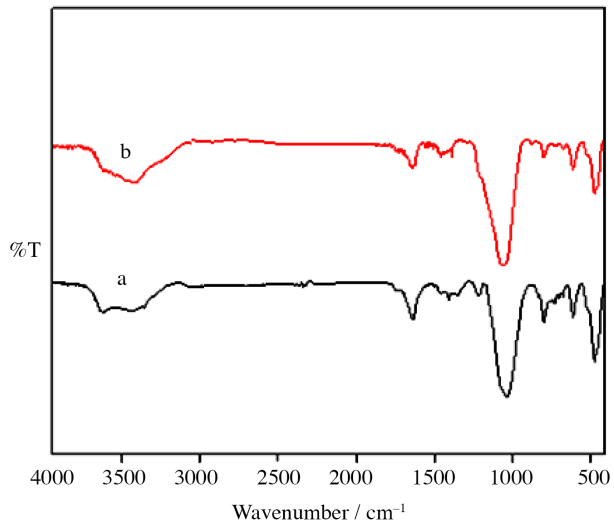

Figure 5. FTIR spectra of a) fresh ($[Cu(dipic)(H_2O)_2]_n$/Y, b) recycled $[Cu(dipic)(H_2O)_2]_n$/Y.

Consistent with Figures 5a and 5b, the recycled catalyst was not damaged and its spectrum was similar to that of fresh catalyst. These recycling results are encouraging when compared to the literature.

On the other hand, a (Cu–Fe)(salen)/Y complex used for the epoxidation of cyclohexene lost activity by 45% after three consequent runs; degradation of the catalyst was even noted from a change in color.[9] A Mn(III)–salen complex immobilized into pillared clays was found to be somewhat unstable.[33]

3. Experimental

3.1. Materials and equipment

The starting materials and solvents were purchased from Merck and used without purification. NaY with a Si/Al ratio of 2.53 was purchased from Aldrich (lot no. 67812).

Elemental analyses were conducted on a CHN PerkinElmer 2400 analyzer. FTIR spectra were recorded on a PerkinElmer 597 spectrometer. The chemical composition was determined with an inductively coupled plasma–atomic emission spectrometer (ICP-Spectro Genesis). XRD patterns were recorded on a Philips PW1130 X-ray diffractometer with Cu Kα target (λ = 1.54 Å). X-band EPR spectra were recorded with a Jeol JES-FA 200S spectrometer at room temperature. The reaction products of the oxidation were analyzed by an HP Agilent 6890 gas chromatograph equipped with an HP-5 capillary column (phenyl methyl siloxane 30 m $\times$ 320 μm $\times$ 0.25 μm) and a flame-ionization detector.

3.2. 2,6-Pyridinedicarboxylic acid (H_2dipic)

2,6-Pyridinedicarboxylic acid (H_2dipic) was purchased from Merck and characterized by FTIR.

FTIR (KBr, cm^{-1}): 3430 (br), 1702 (vs), 1607 (w), 1581 (s), 1341 (s), 1285 (w), 1088 (m), 706 (s).

3.3. Synthesis of $[Cu(dipic)(H_2O)_2]_n$ complex (1)

The complex, $[Cu(dipic)(H_2O)_2]_n$, was synthesized according to the method reported by Xie et al.[10] (Scheme 2).

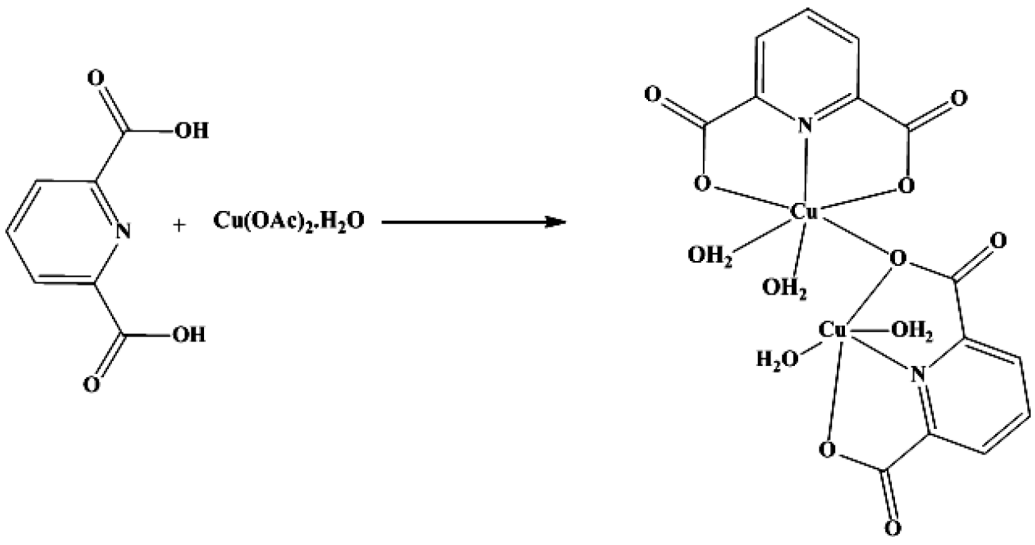

Scheme 2. Schematic representation of the preparation of $[Cu(dipic)(H_2O)_2]_n$ complex.

H_2dipic (2 mmol) dissolved in methanol was added to the solution of $Cu(OAc)_2.H_2O$ (1 mmol) in methanol (5 mL), and the mixed solution was refluxed for 4 h. The green crystals of the title compound were obtained by evaporation for 7 days. $[Cu(dipic)(H_2O)_2]_n$, (M_r = 264.68 g mol^{-1}): Elemental Anal. Calcd. for $C_7H_7CuNO_6$ (%): C, 31.70; H, 2.64; N, 5.82. Found: C, 31.44; H, 2.80; N, 5.69.; Yield: 48%. FTIR (KBr, cm^{-1}): 3444 (br), 1651 (vs), 1618 (s), 1600 (w), 1584 (s), 1374 (s), 1063 (m), 776 (s), 707 (s), 545 (w), 436 (w).

3.4. Preparation of Cu^{II}-exchanged zeolite

Cu–Y was prepared by a conventional ion-exchange method.[34] First 1 g of NaY zeolite was suspended in 25 mL of copper acetate aqueous solution that contained 0.5 mmol of $Cu(OAc)_2$, and the resulting mixture was stirred for 24 h. The solid portion was subsequently filtered, washed with deionized water, and dried at 100 °C overnight to obtain Cu–Y. Analysis of the refluxed solution revealed that approximately 3.66% of copper ions had been exchanged. The obtained Cu–Y was characterized by FTIR spectroscopy, ICP, EPR, and XRD. ICP results for Na–Y: Si, 21.76, Na, 7.5, Al, 8.61%, Si/Al = 2.53.; ICP results for Cu–Y: Si, 21.46, Na, 3.25, Al, 8.46, Cu, 3.66 %, Si/Al = 2.53.

3.5. Preparation of the encapsulated complex (2)

The metal complex was encapsulated in zeolite in several steps. The copper exchanged zeolite described earlier along with a large excess of 2,6-pyridinedicarboxylic acid (1 mmol) was suspended in dichloromethane. The suspension was stirred for 24 h under nitrogen atmosphere. Unchanged ligand and any transition metal complex adsorbed on the external surface of Cu–Y zeolite were removed by Soxhlet extraction with dichloromethane. The extracted product was further ion-exchanged with 0.1 M sodium chloride to remove copper ions. This was washed with deionized water until no chloride ions could be detected (by reaction with silver nitrate). The product dried in air was characterized by FTIR spectroscopy, ICP, EPR, and XRD.

The resulting zeolite-encapsulated product is denoted as $[Cu(dipic)(H_2O)_2]_n$/Y. ICP results for $[Cu(dipic)(H_2O)_2]_n$/Y: Si = 21.05, Na, 5.31, Al, 8.32; Cu, 2.53%. Complex encapsulated = 0.4 mmol g^{-1} zeolite (=2.53%). FTIR (KBr, cm^{-1}): 3640 (b), 3454 (b), 3370 (w), 3090 (w), 1646 (m), 1466 (w), 1410 (w), 1366 (w), 1224 (w), 1042 (vs), 795 (m), 607 (m), 468 (s); CHN results: calculated; $[Cu(dipic)(H_2O)_2]_n$/Y: C, 3.36; H, 0.28; N, 0.56%, Ligand encapsulated = 0.4 mmol g^{-1} zeolite. Found; C, 3.44; H, 0.38; N, 0.56%, Ligand encapsulated = 0.41 mmol g^{-1} zeolite.

3.6. General oxidation procedure

The oxidation reactions of substrates (cyclohexene, cyclohexane, ethyl benzene, and toluene) with hydrogen peroxide were performed in a 25-mL round-bottom flask with a reflux condenser. A mixture of catalyst (4 mg), 2.0 mL of solvent, and 1.0 mmol cyclohexene was stirred at 60 °C. Hydrogen peroxide was also added. After the reaction, the reaction products were quantified by gas chromatography. The products were assigned by comparing their retention times with those of authentic samples. Yields, which are based on the added substrate, were determined by means of a calibration curve.

To investigate the possibility of numerous recycling runs for $[Cu(dipic)(H_2O)_2]_n$/Y, the solid catalyst was separated from the reaction mixture by centrifugation, washed several times with acetonitrile, and then used again in a subsequent reaction.

In a separate experiment to examine the leaching of copper, after 2 h the solid catalyst $[Cu(dipic)(H_2O)_2]_n$/Y was removed from the reaction mixture. The remaining solution was decanted. The concentrated H_2SO_4 was added to the supernatant and then it was refluxed for 2 h. The resulting solution was analyzed by atomic absorption spectroscopy to detect the amount of copper leached from the catalyst.

Acknowledgment

The authors are grateful to the University of Zanjan for its financial support of this study.

References

1. Baca, S. G.; Reetz, M. T.; Goddard, R.; Filippova, I. G.; Simonov, Y. A.; Gdaniec, M.; Gerbeleu, N. *Polyhedron* **2006**, *25*, 1215–1222.
2. Ghorbanloo, M.; Rahmani, S.; Yahiro, H. *Transit. Metal. Chem.* **2013**, *38*, 725–732.
3. Mozgawa, W.; Krol, M.; Pichor, W. *J. Hazard. Mater.* **2009**, *168*, 1482–1489.
4. Kumar Bansala, V.; Protasis Thankachana, P.; Prasad, *R. Appl. Catal. A: Gen.* **2010**, *381*, 8–17.
5. Jin, C.; Fan, W.; Jia, Y.; Fan, B.; Ma, J.; Li, R. *J. Mol. Catal. A: Chem.* **2006**, *249*, 23–30.
6. Ghorbanloo, M.; Hosseini-Monfared, H.; Janiak, C. *J. Mol. Catal. A: Chem.* **2011**, *345*, 12–20.
7. Ghorbanloo, M.; Jaworska, M.; Paluch, P.; Li, G. D.; Zhou, L. *Transit. Metal. Chem.* **2013**, *38*, 511–521.
8. Ghorbanloo, M.; Tarasi, R.; Tao, J.; Yahiro, H. *Turk. J. Chem.* **2014**, *38*, 488–503.
9. Fan, B.; Li, H.; Fan, W.; Jin, C.; Li, R. *Appl. Catal. A: Gen.* **2008**, *340,* 67–75.
10. Xie, C.; Zhang, Z.; Wang, Z.; Liu, X.; Shen, G.; Wang, R.; Shen, D. *J. Coord. Chem.* **2004**, *57*, 1173–1178.
11. Van Albada, G. A.; Haasnoot, J. G.; Reedijk, J.; Biagini-Cingi, M.; Manotti-Lanfredi, A. M.; Ugozzoli, F. *Polyhedron* **1995**, *14,* 2467–2473.
12. Carmona, P. *Spectrochim Acta A-M.* **1980**, *36*, 705–712.
13. Li, W.; Juan, L.; En-bo, W. *Chem. Res. Chinese. U.* **2004**, *20*, 127–130.
14. Nakamoto, K. *Infrared and Raman Spectra of Inorganic and Coordination Compounds*. Wiley, New York, NY, USA 1986.
15. Bloomquist, D. R.; Willet, R. D. *Coord. Chem. Rev.* **1982**, *47*, 125–164.
16. Abraham, R.; Yuseff, K. K. M. *J. Mol. Catal. A, Chem.* **2003**, *198*, 175–183.
17. Bennur, T. H.; Srinivas, D.; Sivasanker, S. *J. Mol. Catal. A: Chem.* **2004**, *207*, 163–171.
18. Kapoor, P.; Pathak, A.; Kapoor, R.; Venugopalan, P.; Corbella, M.; Rodriguez, M.; Robles, J.; Llobet, A. *Inorg. Chem.* **2002**, *41*, 6153–6160.
19. Koval, I. A.; Sgobba, M.; Huisman, M.; Lüken, M.; Saint-Aman, E.; Gamez, P.; Krebs, B.; Reedijk. *J. Inorg. Chim. Acta.* **2006**, *359*, 4071–4078.
20. Alves, W. A.; de Almeida Santos, R. H.; Paduan-Filho, A.; Becerra, C. C.; Borin, A. C.; Da Costa Ferreira, A. M. *Inorg. Chim. Acta.* **2004**, *357*, 2269–2278.
21. Singh, L. J.; Devi, N. S.; Devi, S. P.; Devi, W. B.; Singh, R. K. H.; Rajeswari, B.; Kadam, R. M. *Inorg. Chem. Commun.* **2010**, *13*, 365–368.
22. Hoffmann, S. K.; Towle, D.; Hatfield, W. E.; Chaudhuri, P.; Wieghardt, K. *Inorg. Chem.* **1985**, *24*, 1307–1312.
23. Gelasco, A.; Kirk, M. L.; Kampf, J. W.; Pecoraro, V. L. *Inorg. Chem.* **1997**, *36*, 1829–1837.
24. Salavati-Niasari, M.; Salimi, Z.; Bazarganipour, M.; Davar, F. *Inorg. Chim. Acta* **2009**, *362*, 3715–3724.
25. Parida, K. M.; Sahoo, M.; Singha, S. *J. Catal.* **2010**, *276*, 161–169.

26. Hosseini-Monfared, H.; Kheirabadi, S.; Asghari-Lalami, N.; Mayer, P. *Polyhedron* **2011**, *30*, 1375–1384.
27. de Vos, D.; Bein, T. *Chem. Commun.* **1996**, *8*, 917–918.
28. Jin, C.; Fan, W.; Jia, Y.; Fan, V.; Ma, J.; Li, R. *J. Mol. Catal. A: Chem.* **2006**, *249*, 23–30.
29. Xavier, K. O.; Chacko, J.; Mohammed Yusuff, K. K. *Appl. Catal. A: Gen.* **2004**, *258*, 251–259.
30. Salavati-Niasari, M. *J. Mol. Catal. A: Chem.* **2008**, *284*, 97–107.
31. Salavati-Niasari, M. *J. Mol. Catal. A: Chem.* **2008**, *283*, 120–128.
32. De Vos, D. E.; Dams, M.; Sels, B. F.; Jacobs, P. A. *Chem. Rev.* **2002**, *102*, 3615–3640.
33. Cardoso, B.; Pires, J.; Carvalho, A. P.; Kuzniarska-Biernacka , I.; Silva, A. R.; de Castro, B.; Freire, C. *Micropor. Mesopor. Mater.* **2005**, *86*, 295–302.
34. Farzaneh, F.; Soleimannejad, J.; Ghandi, M. *J. Mol. Catal. A*. **1997**, *118*, 223–227.